Published in final edited form as:

J Immunol. 2022 March 15; 208(6): 1378–1388. doi:10.4049/jimmunol.2100843.

Direct Binding of Rap1 to Talin1 and to MRL Proteins Promotes Integrin Activation in CD4+ T Cells

Frederic Lagarrigue[*], **Boyang Tan**[†], **Qinyi Du**[†], **Zhichao Fan**[‡], **Miguel A. Lopez-Ramirez**[†], **Alexandre R. Gingras**[†], **Hsin Wang**[†], **Weiwei Qi**[†], **Hao Sun**[†]

[*] Institut de Pharmacologie et Biologie Structurale, Université de Toulouse, CNRS, Université Paul Sabatier, Toulouse, France

[†] Department of Medicine, University of California, San Diego, La Jolla, CA

[‡] Department of Immunology, School of Medicine, University of Connecticut, UConn Health, Farmington, CT

Abstract

Agonist-induced Rap1 GTP loading results in integrin activation involved in T cell trafficking and functions. MRL proteins Rap1-interacting adapter molecule (RIAM) and lamellipodin (LPD) are Rap1 effectors that can recruit talin1 to integrins, resulting in integrin activation. Recent work also implicates direct Rap1–talin1 interaction in integrin activation. Here, we analyze in mice the connections between Rap1 and talin1 that support integrin activation in conventional $CD4^+$ T (Tconv) and $CD25^{Hi}Foxp3^+CD4^+$ regulatory T (Treg) cells. Talin1(R35E, R118E) mutation that disrupts both Rap1 binding sites results in a partial defect in $\alpha_L\beta_2$, $\alpha_4\beta_1$, and $\alpha_4\beta_7$ integrin activation in both Tconv and Treg cells with resulting defects in T cell homing. Talin1(R35E,R118E) Tconv manifested reduced capacity to induce colitis in an adoptive transfer mouse model. Loss of RIAM exacerbates the defects in Treg cell function caused by the talin1(R35E,R118E) mutation, and deleting both MRL proteins in combination with talin1(R35E,R118E) phenocopy the complete lack of integrin activation observed in Rap1a/b-null Treg cells. In sum, these data reveal the functionally significant connections between Rap1 and talin1 that enable $\alpha_L\beta_2$, $\alpha_4\beta_1$, and $\alpha_4\beta_7$ integrin activation in $CD4^+$ T cells.

Integrin adhesion receptors play an essential role in lymphocytes to shape a successful adaptive immune response (1, 2). Integrins participate in lymphocyte development and trafficking to lymphoid organs and sites of inflammation (3, 4). In addition, they are instrumental in the formation of immunological synapses to control T cell functions (5), in particular their capacity to detect Ags and kill. Binding of $\alpha_L\beta_2$ (LFA-1, CD11a/CD18), $\alpha_4\beta_1$ (VLA-4), and $\alpha_4\beta_7$ integrins to their cognate ligands is precisely controlled in

Address correspondence and reprint requests to Hao Sun, University of California, San Diego, 9500 Gilman Drive, Leichtag Building, Room 149, La Jolla, CA 92093, has073@ucsd.edu.

Disclosures

The authors have no financial conflicts of interest.

The online version of this article contains supplemental material.

lymphocytes (6, 7), and deregulation in their activity contributes to various diseases, such as multiple sclerosis, asthma, atherosclerosis, and inflammatory bowel disease (8–10).

Integrins in lymphocytes are usually maintained in a low-affinity state until agonist stimulation induces a high-affinity form (11). This process, operationally defined as "integrin activation," is central to T cell functions (6, 7). The capacity of intracellular signaling pathways to induce such changes in integrin conformation and affinity depends on binding of the cytosolic adapter talin1 to the integrin β cytoplasmic tail, which is a critical common final step in integrin activation (12, 13). Talin1 is unique in its ability to regulate activation of β_1 (13), β_2 (14, 15), β_3 (13), and β_7 (16) integrins. Talin1 is a large multidomain protein that links integrins to the actin cytoskeleton via its N-terminal head domain that binds to the integrin β cytoplasmic tail and its C-terminal rod domain that binds F-actin (17, 18). Talin1 head domain comprises an atypical FERM domain characterized by an additional F0 subdomain to the characteristic FERM F1, F2, and F3 subdomains (17). Talin1 is autoinhibited in the cytosol due to the interaction of the talin1 head domain with the rod domain, which prevents its interaction with the integrin β cytoplasmic tail (19). The effects of talin1 deletion in mouse blood cells have unequivocally confirmed its importance in integrin activation in lymphocytes (14, 20–22); however, the sequence of signal transduction events from adhesive stimuli to talin1 recruitment to integrins are not yet fully characterized.

T cell stimulation via chemokines or Ag receptors initiates a cascade of signaling pathways that converge on talin1 to trigger integrin activation (2). Rap1 GTPases function as a prominent signaling hub that controls talin1 binding to T cell integrins (23). Pioneer studies identified Rap1-interacting adapter molecule (RIAM) as a Rap1 effector that recruits talin1 to the plasma membrane to enable its interaction with the integrin β cytoplasmic tail (24). RIAM is abundant in hematopoietic cells (25). In contrast to talin1 deletion (26, 27), germline loss of RIAM in mice does not affect development, hemostasis, or platelet integrin activation and function (28–30). However, RIAM-null mice exhibit significant leukocytosis and impaired integrin-mediated T cell adhesion and homing to lymph nodes (29, 30). Moreover, RIAM plays an essential role in the dynamic regulation of lymphocyte integrin function during the formation of the immunological synapse and killing activity (31). RIAM deficiency results in a loss of β_2 integrin activation in multiple leukocyte subsets, including T cells, whereas activation of $\alpha_4\beta_1$ integrin operates in a RIAM-independent manner (29, 30). In contrast, we showed that RIAM is dispensable for integrin activation and function in regulatory T (Treg) cells despite the fact that Rap1 is required for Treg cell function and RIAM is expressed in Treg cells (32). Increased expression of lamellipodin (LPD), a RIAM paralog, accounts for the lack of RIAM requirement in Treg cells (32). RIAM and LPD are mammalian members of the Mig-10/RIAM/LPD (MRL) protein family; LPD plays a more important role than RIAM in Treg cell integrin activation. Accordingly, targeting RIAM could provide an avenue for cell type–specific inhibition of integrin activation to ameliorate autoimmune disorders such as type 1 experimental diabetes (31) or inflammatory bowel disease (32) by suppressing integrin-mediated homing and function of $CD4^+$ T cells while sparing Treg cells.

Because RIAM deficiency in T cells has a less pronounced effect on leukocyte β_2 integrin function than loss of either talin1 or Rap1 expression (28, 29), the existence of alternative RIAM-independent pathways that regulate Rap1-mediated recruitment of talin1 to T cell integrins becomes evident. Previous studies revealed that Rap1 can bind directly to the talin1 F0 subdomain with low affinity (33, 34). However, blockade of Rap1–talin1 F0 interaction has a relatively minor effect on platelet integrin activation and hemostasis (35, 36). Thereafter, we identified a second Rap1 binding site in the talin1 F1 subdomain of similar affinity to that in F0 (37). Mutation R118E in the talin1 F1 subdomain, which blocks Rap1 binding, abolished the capacity of Rap1 to mediate talin1-induced integrin activation in model Chinese hamster ovary (CHO) cells and platelets (37, 38). Disruption of Rap1 binding to both talin1 F0 and F1 subdomains further impairs integrin activation to an extent similar to that observed in platelets lacking both Rap1a and Rap1b (38). These studies revealed that Rap1 binding to both talin1 F0 and F1 subdomains is crucial for platelet integrin function and hemostasis. In addition to likely facilitating membrane recruitment of talin1 in platelets and endothelial cells, the direct interaction of talin1 with Rap1 can place talin1 in proximity to and in appropriate orientation with plasma membrane phospholipids and the integrin β_3 cytoplasmic tail, leading to integrin activation (39).

Here, we assessed the contribution of the Rap1–talin1 interaction to trigger integrin activation in T cells. We generated mice bearing point mutations in the talin1 F0 subdomain (R35E), F1 subdomain (R118E), or both F0 and F1 subdomains (R35E,R118E) (35, 38). Mutation R35E or R118E to disrupt Rap1 binding to either the talin1 F0 or F1 subdomains, respectively, cause a significant but moderate defect in $\alpha_L\beta_2$, $\alpha_4\beta_1$, and $\alpha_4\beta_7$ integrin activation in $CD4^+$ T cells. T cells expressing the talin1(R35E,R118E) mutant manifest further impaired integrin activation and exhibit reduced capacity to induce colitis in an adoptive transfer model. Overexpression of RIAM in mutant T cells expressing talin1(R35E,R118E) restored the capacity of Rap1 to potentiate integrin activation. In contrast, loss of RIAM in talin1 (R35E,R118E) mutant T cells exacerbate the defects in integrin activation. Thus, direct binding of Rap1 to talin1 operates as an alternative pathway to the Rap1–RIAM axis to control integrin activation in $CD4^+$ T cells. Similarly, Rap1–talin1 interaction participates, in parallel with LPD, in $\alpha_L\beta_2$ and $\alpha_4\beta_7$ integrin function in Treg cells. These data reveal the contribution of multiple routes that connect Rap1 to talin1 in Treg and $CD4^+$ T cells and highlight the potential of interfering with these pathways to specifically manipulate the trafficking and function of selective lymphocyte subsets to ameliorate autoimmunity.

Materials and Methods

Abs and reagents

The following Abs were from BioLegend: CD3 (17A2, 2C11), CD4 (GK1.5), CD29 (HMb1–1), CD49d (R1–2), β_7 integrin (FIB504), and Foxp3 (MF-14). Ab against RIAM was from R&D Systems. Abs against talin1 (8d4; Sigma-Aldrich), RIAM (produced in rabbits immunized with recombinant 1–301 portion of human RIAM), Rap1 (sc-398755; Santa Cruz Biotechnology), and β-actin (A5316; Sigma-Aldrich) were used for Western blot analysis. Secondary Abs conjugated to Alexa Fluor were from Jackson ImmunoResearch.

eFluor 670 was from BioLegend. PMA was from Sigma-Aldrich. The MojoSort mouse CD4 T cell isolation kit was from BioLegend. Liberase TL (Research Grade) and DNase I were from Roche. All adhesion molecules (ICAM-1, VCAM-1, and MAdCAM-1) are fused with a human IgG1 Fc tag at the C terminus. Recombinant mouse ICAM-1-Fc and VCAM-1-Fc were from BioLegend. Recombinant mouse MAdCAM-1-Fc was from R&D Systems.

Mice

All animal experiments were approved by the institutional animal care and use committee of the University of California, San Diego, and were conducted in compliance with federal regulations as well as institutional guidelines and regulations pertaining to animal studies. *Apbb1ip*$^{Flox/Flox}$ (28, 29), *Tln1*$^{Flox/Flox}$ (26), *Tln1*$^{wt/R35E}$ (35), *Tln1*$^{wt/R118E}$ (38), *Tln1*$^{wt/R35E,R118E}$ (38), *Rap1a/b*$^{Flox/Flox}$ (29), *Tln1*$^{wt/L325R}$ (40), *Raph1*$^{Flox/Flox}$ (41), *CD4*^{Cre} (42), and *Foxp3*$^{YFP\text{-}Cre}$ (43) mice have been described previously. Hemizygous mice with point mutations in *Tln1* were crossed with *Tln1*$^{Flox/Flox}$; *CD4*^{Cre} to obtain lymphocyte-specific deletion of *Tln1* flox allele in *Tln1*$^{Flox/wt}$; *CD4*^{Cre} (control) and *Tln1*$^{Flox/Mutation}$; *CD4*^{Cre} littermates for experiments. Similarly, *Tln1*$^{Flox/wt}$; *Foxp3*$^{YFP\text{-}Cre}$ (control) mice were compared with *Tln1*$^{Flox/Mutation;}$ *Foxp3*$^{YFP\text{-}Cre}$ littermates for experiments. RIAM conditional knockout RIAM-cKO refers to *Apbb1ip*$^{Flox/Flox}$; *CD4*^{Cre} mice, and RIAM conditional knockout RIAM-rKO refers to *Apbb1ip*$^{Flox/Flox}$; *Foxp3*$^{YFP\text{-}Cre}$ mice. Similarly, LPD-rKO refers to *Raph1*$^{Flox/Flox}$; *Foxp3*$^{YFP\text{-}Cre}$ mice. All mice were from a mixed C57BL/6-Sv129 or -SJL genetic background. All individual strains have been backcrossed more than five times to the C57BL/6J strain before proceeding to outcrosses between strains. Eight- to twelve-week-old, sex-matched wild-type (WT) littermates were used as control animals for all experiments. All mice were housed in specific pathogen-free conditions.

Blood counts

Peripheral blood was collected from the retro-orbital plexus into tubes containing K^+/EDTA. Cell counts were performed using a Hemavet 950FS Hematology System programmed with mouse-specific settings (Drew Scientific). All samples were tested in duplicate, and the mean for each animal was plotted.

T cell purification

T cells were isolated from spleens as previously described (32). Briefly, $CD4^+$ T cells were purified by magnetic separation using the $CD4^+$ T cell negative isolation kit (BioLegend) and were routinely >95% $CD3^+$ by flow cytometry. $CD4^+CD25^-CD45^{RBhigh}$ T_{conv} were purified by adding a biotinylated anti-CD25 Ab (PC61; BioLegend) to the $CD4^+$ T cell negative isolation kit to deplete Treg cells. YFP^+ Treg cells were sorted with a FACSAria II cytometer (BD Biosciences).

T cell transduction

Human RIAM cDNA was fused to enhanced GFP (EGFP) at the C terminus and inserted downstream of the murine EF1α promoter into the murine stem cell virus (pMSCV) retroviral backbone using InFusion cloning (Clontech) between the EcoRI and ClaI sites. Primers used were as follows: RIAM

forward: 5′-GTGACCGGCGCCTACGAATTCACCATGGGTGAGTCAAGTGAAGAC-3′; RIAM reverse primer: 5′-CGCCACCTCCGGACACGTTGCCTCTCTTCT-3′; EGFP forward primer: 5′-CAACGTGTCCGGAGGTGGCGGCCGCGGAATGGTGAGCAAGGGCGAGG-3′; EGFP reverse primer: 5′-TAAAATCTTTTATTTTATCGATTTACTTGTACAGCTCGTCCATG-3′. 293-LVX cells (Clontech) were transfected with pMSCV and pCl-Eco using Lipofectamine 3000 (Invitrogen) and cultured for 3 d. Purified $CD4^+$ T cells were activated with immobilized anti-CD3 mAb (145–2C11 clone, 5 μg/ml), anti-CD28 mAb (37.51 clone, 5μg/ml), and IL-2 (20U/ml) in RPMI media for 2 d. Then the cells were washed, mixed with 50% viral supernatant and 50% fresh RPMI medium supplemented with 20U/ml IL-2, and spinfected on RetroNectin (Takara)-coated plates at 3000 ×g at 32°C for 2h. After 1 d, the transduction step was repeated. The next day, cells were washed and maintained in culture between 8×10^5 and 1×10^6 cells/ml with IL-2 (20 U/ml). Cells were assayed for transduction efficiency and function by flow cytometry 2–3 d after the second transduction.

Flow cytometry

Cells isolated from mouse tissues were washed and resuspended in PBS containing 0.1% BSA and stained with conjugated Ab for 30 min at 4°C. Then, cells were washed twice before data acquisition. Intracellular staining with anti-RIAM Ab was performed in 0.5% saponin after fixation with 2% formaldehyde. For soluble ligand binding assay, 5×10^6 cells were washed and resuspended in HBSS containing 0.1% BSA and 1 mM Ca^{2+}/Mg^{2+} before incubation with integrin ligands (5 μg/ml) for 30 min at 37°C with or without 100 nM PMA. Cells were then incubated with Alexa Fluor 647–conjugated anti-human IgG (1:200) for 30 min at 4°C to detect the Fc tag fused to the integrin ligands. Specific binding was calculated as the change in mean fluorescence intensity (ΔMFI; $F - F_0$), in which F is the MFI of soluble ligand binding and F_0 is the MFI in the presence of 5 mM EDTA to measure background binding. We normalized the data to the control condition in the absence of stimulation. Flow cytometric analysis was performed using an Accuri C6 Plus device (BD Biosciences). Data were analyzed using FlowJo software.

Flow chamber assay

Polystyrene Petri dishes were coated with murine VCAM-1/Fc, ICAM-1/FC, or MAdCAM-1/Fc (10 μg/ml) alone or with CXCL12 (SDF1α 1 μg/ml) or P-selectin (10 μg/ml) in coating buffer (PBS, 10 mM $NaHCO_3$, pH 9.0) for 1 h at room temperature, blocked for 1 h with BSA (1%), and then assembled into the flow chamber device (GlycoTech). Cells were diluted to 5×10^6 cells/ml in HBSS (with 1 mM Ca^{2+}/Mg^{2+}) and immediately perfused through the flow chamber at a constant flow of 2 dyn/cm^2. For the PMA stimulation, cells were prestimulated for 10 min with PMA (100 nM) at 37°C before perfusion. Adhesive interactions between the flowing cells and the coated substrates were assessed by manually tracking the motions of individual cells for 1 min as previously described (44). Cells that remained adherent and stationary after the initial adhesion point for >10 s with a velocity <1 μm/s were defined as arrested adherent cells.

T cell proliferation assay

Flat-bottomed 96-well plates were coated overnight at 4°C with anti-CD3 mAb (145–2C11 clone, 5 μg/ml) and anti-CD28 mAb (37.51 clone, 5μg/ml). $CD4^+$ T cells were isolated from the spleen, then labeled with CFSE, seeded at a density of 10^7 cells/ml, and cultured for 4 d at 37°C. The proliferation index was calculated using FlowJo version 10 software.

In vivo competitive lymphocyte homing

Mutant and WT T cells were labeled with 1 or 10μM CFSE, respectively, resulting in readily discriminated cell populations. Equal numbers (1×10^7) of differentially labeled cells were mixed and then injected i.v. into C57BL/6 recipient mice. Lymphoid organs were harvested 3 h after injection, and isolated cells were analyzed by flow cytometry for the ratio of mutant ($CFSE^{lo}$) to WT ($CFSE^{hi}$) T cells in various lymphoid organs.

Treg suppression assay

$CD4^+CD25^-$ T cells (responder cells) were isolated from spleens of C57BL/6 (CD45.1) WT mice. Responder cells were labeled with CFSE and cocultured with YFP^+ Treg cells (8:1, 4:1, 2:1, and 1:1 ratios) in the presence of 5 μg/ml immobilized anti-CD3 mAb (145–2C11 clone, 5 μg/ml), anti-CD28 mAb (37.51 clone, 5μg/ml), and IL-2 (100 U/ml) for 4 d at 37°C. The proliferation index was calculated using FlowJo version 10 software.

Mouse colitis models

Eight- to ten-week-old mice were challenged with an adoptive T cell transfer model. $CD4^+CD25^-CD45^{RBhigh}$ T_{conv} cells (5×10^5) from Tln1-cR35E, R118E or control mice were injected i.p. into *Rag1*$^{-/-}$ mice. Murine body weight was measured daily. Mice were sacrificed at Day 100 after the infusion.

Western blotting

Isolated $CD4^+$ T cells and sorted Treg cells were pelleted by centrifugation at $700 \times g$ for 5 min at room temperature and then lysed in Laemmli sample buffer. Lysates were subjected to 4–20% gradient SDS-PAGE. The appropriate IRDye/Alexa Fluor–conjugated secondary Abs were from LI-COR Biosciences. Nitrocellulose membranes were scanned using an Odyssey CLx infrared imaging system (LI-COR Biosciences), and blots were processed using Image Studio Lite software (LI-COR Biosciences).

Statistical analysis

Statistical significance was assayed by a two-tailed *t* test for single comparisons. ANOVA with a Bonferroni post hoc test was used to assay statistical significance for multiple comparisons. All datasets were tested for Gaussian normality distribution. Statistical analysis was performed using Prism software (version 8.0; GraphPad Software). A p value <0.05 was considered significant.

Results

Rap1 binding to the talin1 F0 or F1 subdomain contributes to integrin activation in CD4+ T cells

We previously generated knock-in mouse strains harboring the point mutations R35E and R118E in the talin1 F0 and F1 subdomains (Fig. 1A), respectively, to disrupt binding to Rap1 (35, 38). We crossed *Tln1*$^{WT/R35E}$;*CD4-Cre*$^{+/-}$ mice with the *Tln1*$^{Flox/Flox}$ strain to T cell–specific deletion of the *Tln1* flox allele in *Tln1*$^{WT/Flox}$;*CD4-Cre*$^{+/-}$ (control) and *Tln1*$^{R35E/Flox}$;*CD4-Cre*$^{+/-}$ (indicated as Tln1-cR35E) littermates for experiments. Similarly, *Tln1*$^{R118E/Flox}$;*CD4-Cre*$^{+/-}$ mice (indicated as Tln1-cR118E) were compared with *Tln1*$^{WT/Flox}$;*CD4-Cre*$^{+/-}$ (control) littermates for experiments. *Tln1*$^{WT/R35E}$;*CD4-Cre*$^{+/-}$ and *Tln1*$^{R118E/Flox}$;*CD4-Cre*$^{+/-}$ progenies selectively express talin1(R35E) or talin1(R118E)mutant proteins in T cells. These mutant mice were viable, exhibited no gross developmental defects, and appeared healthy. Lymphocyte expression of talin1, Rap1a/b, and RIAM was unchanged (Supplemental Fig. 1A). Surface expression of α_L, β_2, α_4, β_1, and β_7 integrins in Tln1-cR35E and Tln1-cR118E mice was similar to control T cells (Supplemental Fig. 1B). These data indicate that both Tln1-cR35E and Tln1-cR118E mice are suitable for examination of the effects of blocking Rap1 binding to the talin1 F0 and F1 subdomains on T cell integrin activation and function.

We next measured binding of CD4$^+$ T cells to soluble ICAM-1 (22), VCAM-1 (45), and MAdCAM-1 (16) to assess the activation of $\alpha_L\beta_2$, $\alpha_4\beta_1$, and $\alpha_4\beta_7$ integrins, respectively (Fig. 1B–1D). Tln1-cR35E T cells exhibited a significant reduction in ICAM-1 (Fig. 1B) and MAdCAM-1 (Fig. 1D) binding upon stimulation with PMA. This defective binding was even more pronounced in Tln1-cR118E T cells. In sharp contrast, binding of mutant T cells to VCAM-1 was similar to that in control cells (Fig. 1C). Thus, these findings indicate that blockade of Rap1 binding to talin1 F0 or F1 subdomains partially inhibits activation of $\alpha_L\beta_2$ and $\alpha_4\beta_7$ integrins while preserving activation of $\alpha_4\beta_1$ integrin.

Blockade of Rap1 binding to both talin1 F0 and F1 subdomains markedly reduces integrin activation in CD4+ T cells

To assess the contribution of Rap1–talin1 interaction in T cells (Fig. 2A), we crossed *Tln1*$^{WT/R35E,R118E}$;*CD4-Cre*$^{+/-}$ mice (38) with the *Tln1*$^{Flox/Flox}$ strain to obtain lymphocyte-specific deletion of *Tln1* flox allele in *Tln1*$^{WT/Flox}$;*CD4-Cre*$^{+/-}$ (control) and *Tln1*$^{R35E,R118E/Flox}$; *CD4*-Cre$^{+/-}$ (indicated as Tln1-cR35E,R118E) littermates for experiments. The lymphocyte content of talin1, RIAM, and Rap1a/b (Supplemental Fig. 1C) and surface expression of α_L, β_2, α_4, β_1, and β_7 integrins (Supplemental Fig. 1D) in Tln1-cR35E,R118E T cells were similar to those in WT T cells. Tln1-cR35E,R118E mice were viable, appeared healthy, and exhibited normal counts of leukocytes in peripheral blood (Fig. 2B). Binding of PMA-stimulated Tln1-cR35E, R118E T cells to ICAM-1 and MAdCAM-1 was strongly reduced when compared with that in control T cells (Fig. 2C). Similarly, binding of Tln1-cR35E,R118E T cells to VCAM-1 was impaired (Fig. 2C), indicating that complete blockade of Rap1 binding to talin1 regulates $\alpha_4\beta_1$ activation in addition to activation of $\alpha_L\beta_2$ and $\alpha_4\beta_7$ integrins. Accordingly, adhesion of Tln1-cR35E,R118E T cells onto the three integrin ligands was impaired upon stimulation with either PMA

or SDF1α under a flow condition (Fig. 2D). Because talin1 plays an important role in integrin-mediated trafficking of lymphocytes to lymph nodes (16, 46), we performed a competitive homing assay to measure the capacity of Tln1-cR35E,R118E T cells to migrate in vivo (Fig. 2E). Tln1-cR35E,R118E T cells manifested reduced homing to both mesenteric lymph nodes (MLNs) and peripheral lymph nodes (PLNs) (Fig. 2F). In addition, Tln1-cR35E,R118E T cells exhibited a mild but significant reduction in proliferation upon exposure to anti-CD3/CD28 (Fig. 2G). Thus, disruption of the Rap1–talin1 interaction profoundly impairs integrin activation and function in $CD4^+$ T cells.

Talin1 R35E and R118E mutations in $CD4^+$ T cells reduced their capacity to induce colitis

Because the Tln1-cR35E,R118E mice were apparently healthy, yet exhibited defects in T cell integrin activation, we hypothesized that mutated T cells might lack the capacity to provoke autoimmune inflammation. We induced experimental autoimmune colitis (32) by infusing $CD4^+CD25^-CD45^{RBhigh}$ T cells (T_{conv}) from Tln1-cR35E,R118E mice or WT control mice into *Rag1*$^{-/-}$ recipient mice. *Rag1*$^{-/-}$ mice injected with WT T_{conv} exhibited a progressive loss in bodyweight 30–50 d after the infusion (Fig. 3A). Forty percent of these mice died by Day 100 (Fig. 3B). In contrast, *Rag1*$^{-/-}$ mice injected with Tln1-cR35E,R118E T_{conv} exhibited a small loss of body weight, and only 15% of these mice died by Day 100 (Fig. 3A, 3B). The difference in inflammatory cell infiltration between Tln1-cR35E,R118E and WT T_{conv} infused *Rag1*$^{-/-}$ mice was confirmed by the reduction in colonic expression of proinflammatory cytokines (IL-1β, TNF-α, IL-6, IFN-γ, and IL-17A) in Tln1-cR35E,R118E T_{conv} recipients (Fig. 3C). Thus, the defect in integrin activation in Tln1-cR35E,R118E $CD4^+$ T cells is associated with impaired capacity to induce intestinal inflammation.

Both RIAM and Rap1 binding to talin1 operate in $CD4^+$ T cells to regulate integrin activity

Because blockade of Rap1–talin1 interaction partially diminished integrin activation in Tln1-cR35E,R118E T cells, we reasoned that additional routes linking Rap1 to talin1 are involved in $CD4^+$ T cells. RIAM is a member of the MRL family of adapter proteins that participate in cell migration by controlling integrin activation and dynamics of the actin cytoskeleton (24, 25, 47, 48). We hypothesized that RIAM and talin1 together contributed to the capacity of Rap1 to promote integrin activation in $CD4^+$ T cells (Fig. 4A). We crossed the Tln1-cR35E,R118E mice with the RIAM-cKO strain, which is null for RIAM expression. *Tln1*$^{R35E,R118E/Flox}$*;Apbb1ip*$^{Flox/Flox}$*; CD4-Cre*$^{+/-}$ mice (indicated as Tln1-cR35E,R118E; RIAM-cKO) were compared with *Tln1*$^{WT/Flox}$*;Apbb1ip*$^{WT/WT}$*;CD4-Cre*$^{+/-}$ (control) littermates for experiments. These mutant mice were viable and apparently healthy, and their $CD4^+$ T cells expressed a normal complement of talin1 and Rap1a/b (Supplemental Fig. 1E) or α_L, β_2, α_4, β_1, and β_7 integrins (Supplemental Fig. 1F) when compared with control cells. Tln1-cR35E,R118E; RIAM-cKO T cells exhibited a substantial reduction in their capacity to home to PLNs and MLNs (Fig. 4B). In agreement with previous reports (28, 32), we observed impaired binding of RIAM-deficient $CD4^+$ T cells to ICAM-1 and MAdCAM-1 in response to PMA stimulation, whereas defects in binding to VCAM-1 were minimal (Fig. 4C). The reduction in integrin ligand binding was greater in Tln1-cR35E,R118E T cells. These defects were even more dramatic in Tln1-cR35E,R118E; RIAM-cKO T cells in which binding to ICAM-1 and MAdCAM-1 was

completely abolished (Fig. 4C), thus mimicking the effect of Rap1a/b deletion. Accordingly, $CD4^+$ T cells from RIAM-cKO, Tln1-cR35E, R118E, and Tln1-cR35E,R118E; RIAM-cKO mice showed a graduated defect in adhesion in shear flow upon stimulation with SDF1α or PMA (Supplemental Fig. 3). Thus, the combination of Rap1 binding to talin1 and to RIAM can account for the effect of Rap1 in $CD4^+$ T cell integrin activation.

We reasoned that if talin1 or RIAM could connect Rap1 to integrins (Fig. 4A), then RIAM might be able to bridge Rap1 to talin1 (R35E,R118E), thereby compensating for the loss of direct Rap1 binding to talin1(R35E,R118E). We therefore tested whether increasing RIAM expression in Tln1-cR35E,R118E $CD4^+$ T cells can restore the activation defects of $\alpha_L\beta_2$, $\alpha_4\beta_1$, and $\alpha_4\beta_7$ integrins. We transduced proliferating Tln1-cR35E,R118E $CD4^+$ T cells with MSCV retroviruses encoding either RIAM-IRES-EGFP or EGFP alone. Overexpression of RIAM in Tln1-cR35E,R118E T cells fully restored activation of $\alpha_L\beta_2$, $\alpha_4\beta_1$, and $\alpha_4\beta_7$ integrins (Fig. 4D, 4E). These data demonstrate that both the Rap1–RIAM axis and Rap1 binding to talin1 contribute to integrin activation in $CD4^+$ T cells, with Rap1–talin1 interaction making a greater contribution, and that RIAM can compensate for the defect in integrin action in Tln1-cR35E,R118E $CD4^+$ T cells.

Rap1–talin1 interaction participates in integrin activation in Treg cells

We previously reported that distinct integrin activation pathways operate in effector and Treg cells (32). We crossed $Tln1^{WT/R35E,R118E}$ mice with $Foxp3^{YFP\text{-}Cre}$ mice to generate $Tln1^{WT/R35E,R118E}$;$Foxp3^{YFP\text{-}Cre}$ mice in which the Cre recombinase is selectively expressed in Treg cells. We next crossed $Tln1^{WT/R35E,R118E}$;$Foxp3^{YFP\text{-}Cre}$ mice with the $Tln1^{Flox/Flox}$ strain to obtain Treg cell–specific deletion of the *Tln1* flox allele in $Tln1^{WT/Flox}$;$Foxp3^{YFP\text{-}Cre}$ (control) and $Tln1^{R35E,R118E/Flox}$; $Foxp3^{YFP\text{-}Cre}$ (indicated as Tln1-rR35E,R118E) littermates for experiments (Fig. 5A). Expression of talin1(R35E,R118E), RIAM and Rap1a/b was unaffected in Tln1-rR35E,R118E Treg cells when compared with $Tln1^{WT/Flox}$;$Foxp3^{YFP\text{-}Cre}$ control Treg cells (Supplemental Fig. 2A), and surface levels of α_L, β_2, α_4, β_1, and β_7 integrins were intact (Supplemental Fig. 2B). Tln1-rR35E,R118E mice manifested a significant leukocytosis (Fig. 5B), which mirrors a previous observation that loss of talin1 function in Treg cells causes systemic inflammation (20, 21). Binding of ICAM-1 and MAdCAM-1 to PMA-stimulated Tln1-rR35E,R118E Treg cells was diminished by 50%, whereas binding of VCAM-1 was similar to control Treg cells (Fig. 5C). Consistent with impaired integrin activation, Tln1-rR35E, R118E Treg cells homed less efficiently to PLNs and MLNs (Fig. 5D). Because both Rap1 and talin1 are required to exert suppressive function in Treg cells, we next performed an in vitro suppression assay (Fig. 5E). We observed that Tln1-rR35E,R118E Treg cells exhibited reduced capacity to suppress proliferation of conventional T cells (Fig. 5F). Together, our findings reveal that Rap1–talin1 interaction in Treg cells contributes to the activation and associated functions of $\alpha_L\beta_2$ and $\alpha_4\beta_7$ integrins, whereas, unlike in $CD4^+$ T cells, $\alpha_4\beta_1$ activity is preserved.

RIAM and LPD complement Rap1–talin1 interaction in promoting integrin activation and function in Treg cells

RIAM deficiency has a minor effect on Treg cell integrin activation and function (32). To ask whether Rap1 binding to talin1 supports integrin activation in RIAM-null Treg cells, we generated *Tln1*$^{R35E,R118E/Flox}$;*Apbb1ip*$^{Flox/Flox}$;*Foxp3*$^{YFP\text{-}Cre}$ mice (indicated as Tln1-rR35E,R118E; RIAM-rKO) and *Tln1*$^{WT/Flox}$;*Apbb1ip*$^{WT/WT}$; *Foxp3*$^{YFP\text{-}Cre}$ (control) littermates for experiments. Tln1-rR35E, R118E; RIAM-rKO Treg cells express a level of talin1 similar to that in *Tln1*$^{WT/Flox}$; *Foxp3*$^{YFP\text{-}Cre}$ Treg cells and equal content of Rap1a/b (Supplemental Fig. 2C) or surface α_L, β_2, α_4, β_1, and β_7 integrins (Supplemental Fig. 2D) when compared with control Treg cells. Tln1-rR35E,R118E; RIAM-rKO mice were viable; however, they exhibited a reduced body size when compared with control mice (Fig. 6A) and manifested larger lymph nodes and spleens but smaller thymi (Fig. 6B), suggesting that these mice experienced immune dysregulation. Treg cells isolated from Tln1-rR35E,R118E; RIAM-rKO mice showed reduced binding to ICAM-1 and MAdCAM-1 after PMA stimulation to an extent similar to that observed in Tln1-R35E, R118E Treg cells (Fig. 6C). However, Tln1-rR35E,R118E; RIAM-rKO Treg cells also exhibited a 50% reduction in binding to VCAM-1, explaining why loss of RIAM could impact the function of Tln1-rR35E,R118E Treg cells (Fig. 6C). In contrast, *Apbb1ip*$^{Flox/Flox}$; *Foxp3*$^{YFP\text{-}Cre}$ mice (indicated as RIAM-rKO) displayed normal binding to soluble integrin ligands (Fig. 6C) as previously described (32). Moreover, Treg cells lacking Rap1–talin1 interaction and RIAM were not able to suppress the proliferation of conventional T cells (Fig. 6D) and homed less to PLNs and MLNs (Fig. 6E). These data suggest that although RIAM is dispensable for integrin activation in Treg cells, it complements the direct binding of talin1 to Rap1 in supporting Treg functions.

The foregoing results indicate that direct binding of Rap1 to talin1 is important in Treg and $CD4^+$ T cell integrin activation; however, the MRL proteins RIAM and LPD can also subserve this function. Furthermore, in $CD4^+$ T cells, RIAM and talin1 together can completely account for the capacity of Rap1 to support integrin activation. Because of LPD's importance in Treg cells, we generated *Tln1*$^{R35E,R118E/Flox}$;*Apbb1ip*$^{Flox/Flox}$;*Raph1*$^{Flox/Flox}$;*Foxp3*$^{YFP\text{-}Cre}$ mice (indicated as Tln1-rR35E,R118E; RIAM-rKO; LPD-rKO) and *Tln1*$^{WT/Flox}$;*Apbb1ip*$^{WT/WT}$;*Raph1*$^{WT/WT}$;*Foxp3*$^{YFP\text{-}Cre}$ (control) littermates for experiments. Tln1-rR35E,R118E; RIAM-rKO; LPD-rKO Treg cells exhibited a complete loss of activation of $\alpha_4\beta_1$, $\alpha_L\beta_2$, and $\alpha_4\beta_7$ integrins (Fig. 6F). The defects were similar to those observed in Treg cells lacking Rap1a/b (indicated as Rap1a/b-rKO) or isolated from *Tln1*$^{L325R/Flox}$;*Foxp3*$^{YFP\text{-}Cre}$ mice (indicated as Tln1-rL325R) harboring a mutation (40, 49) that blocks talin1's capacity to activate integrins (Fig. 6F). Taken together, these results establish that the combination of direct binding of Rap1 to talin1 with LPD and RIAM can account for the role of Rap1 in integrin function in Treg cells.

Discussion

Rap1 is a major convergence point of the lymphocyte signaling pathways that result in talin1 binding to the integrin β cytoplasmic tail and subsequent integrin activation to shape a

successful immune response. Although the contribution of RIAM, which is a Rap1 effector, to trigger talin1-dependent activation of T cell integrins is well documented (28, 29, 31, 32, 48), the nature of the connection between Rap1 and talin1 in lymphocytes remains incompletely characterized. We recently identified two Rap1 binding sites in the talin1 F0 and F1 subdomains and generated mice bearing the two point mutations, R35E and R118E, in the talin1 F0 and F1 subdomains, respectively, which block binding to Rap1 (35, 37, 38). Here, we assessed the contribution of the Rap1–talin1 interaction to trigger integrin activation in T cells, and we report a thorough analysis of the dialogue between Rap1 and talin1 in conventional $CD4^+$ lymphocytes or Treg cells. Disruption of Rap1 binding to talin1 causes a significant but moderate defect in $\alpha_L\beta_2$, $\alpha_4\beta_1$, and $\alpha_4\beta_7$ integrin activation in $CD4^+$ T cells. In the absence of Rap1–talin1 interaction, a defect in lymphocyte trafficking is associated with the inability of T cells to provoke experimental colitis in an adoptive transfer model. Furthermore, RIAM-null T cells expressing the talin1(R35E,R118E) mutant manifest further impaired integrin activation. Inversely, overexpression of RIAM restored the capacity of the talin1(R35E,R118E) mutant to mediate integrin activation. Similarly, Rap1–talin1 interaction participates, in parallel with the Rap1–LPD–talin1 axis but not the Rap1–RIAM–talin1 axis, in $\alpha_L\beta_2$ and $\alpha_4\beta_7$ integrin function in Treg cells. These data reveal the contribution of multiple routes that connect Rap1 to talin1 in Treg and $CD4^+$ T cells.

Blockade of Rap1 binding to the talin1 F0 or F1 subdomains partially inhibits activation of $\alpha_L\beta_2$ and $\alpha_4\beta_7$ integrins in T cells, whereas the loss of both Rap1 binding sites further impairs integrin activation. This finding is consistent with our previous observation that disabling both Rap1 binding sites in the F0 and F1 subdomains had a greater effect than hindering F0 or F1 alone (38). Likewise, Bromberger and colleagues reported that a talin1 knock-in mouse strain ($Tln1^{3mut}$), which carries mutations in the talin1 F0 subdomain to block Rap1 binding, manifests mild defects in platelet integrin functions (36), similar to mice expressing the talin1(R35E) mutant (35). Furthermore, blockade of the Rap1–talin1 F0 interaction led to normal blood cell counts in the peripheral blood of talin1(R35E)-expressing mice (35) or $Tln1^{3mut}$ mice (36). In addition, neutrophils from the $Tln1^{3mut}$ mouse have a mild adhesion defect and manifest a partial reduction in blood extravasation (36). However, talin1(R118E)-expressing mice with loss of the Rap1 binding site in talin1 F1 alone exhibit significant leukocytosis that affects both neutrophils and lymphocytes (38). In sum, these data suggest that the Rap1–talin1 F1 interaction has a greater functional impact than the Rap1–talin1 F0 interaction; however, both Rap1 binding sites in talin1 F0 and F1 cooperate to potentiate integrin function in T cells.

Loss of Rap1–talin1 interaction binding did not affect the activation of integrin $\alpha_4\beta_1$ in Treg cells and led to a partial defect in $CD4^+$ T cells, unlike $\alpha_L\beta_2$ and $\alpha_4\beta_7$. Previous studies demonstrated that deletion of RIAM in T cells partially suppressed $\alpha_L\beta_2$ and $a_4\beta_7$ integrin activation but did not block activation of $\alpha_4\beta_1$ (28, 29, 32). In sharp contrast, deletion of either both Rap1a and Rap1b isoforms or talin1 profoundly suppressed activation of $\alpha_4\beta_1$ in addition to the other two integrins (28, 29). The loss of integrin activation was correlated with a loss of homing of these mutant T cells to PLNs. Lymphocytes enter lymph nodes (such as PLNs and MLNs) by rolling, firm adhesion, and diapedesis through the specialized high endothelial venules. Integrin function contributes to each of these steps. In contrast to leukocyte homing in PLNs and MLNs, the spleen lacks high endothelial venules, the

mechanisms that regulate cell trafficking are poorly defined, and the role of integrins is much less important in migration toward the splenic white pulp (50, 51). Accordingly, homing of mutant T cells to the spleen was normal. In addition, these data indicate that another Rap1 effector is involved in β_1 integrin activation. RAPL is a Rap1 effector that regulates the activity of $\alpha_L\beta_2$ integrin through binding to the α_L cytoplasmic tail (52, 53). It appears to regulate kindlin-3 rather than talin1 (54). Previous studies have shown that RAPL-deficient T lymphocytes had impaired adhesion to VCAM-1 upon stimulation with CCL21 despite having a normal surface expression of VLA-4. In addition, RAPL-deficient T lymphocytes also showed defective abilities of homing to PLNs and trafficking to spleens, which require activation of $\alpha_L\beta_2$ and $\alpha_4\beta_1$ (53). RAPL deficiency also inhibited cell adhesion to VCAM-1 in the human T cell line Molt-4 (55). Taken together, these findings raise the possibility that RAPL contributes to the activation of integrin $\alpha_4\beta_1$ while compensating for the lack of RIAM and Rap1–talin1 interaction in T cells. Additional studies are required to address this point and establish the relative importance of each talin1-dependent signaling module with respect to the RAPL pathway.

Overall, our study reveals that the Rap1–RIAM–talin1 axis is partially redundant with the Rap1–talin1 interaction in $CD4^+$ T cells. In line with our observations, Bromberger and colleagues recently reported a concerted action of the two pathways to efficiently recruit talin1 during the initial step of β_2 integrin inside-out signaling in $CD4^+$ T cells and neutrophils (56). In contrast, we showed that RIAM is dispensable in Treg cells (32). Instead, the Rap1–LPD–talin1 axis functions in parallel to the Rap1–talin1 interaction in Treg cells. In conclusion, our findings reveal that although both Rap1 and talin1 are essential for blood cell integrin functions, their connection differs in a cell type–specific manner. These differences embody potential avenues to manipulate the functions and trafficking of particular lymphocyte subsets for fine tuning the immune response.

Supplementary Material

Refer to Web version on PubMed Central for supplementary material.

Acknowledgments

We thank Dr. Mark H. Ginsberg for helpful discussions, support, and critical reading of the manuscript. We acknowledge Dr. Christopher Kit Bonin and Dr. Geneva Hargis from UConn Health School of Medicine for help in the scientific writing and editing of this manuscript.

This work was supported by the American Heart Association Career Development Award 18CDA34110228 (F.L.), the European Union's Horizon 2020 Framework Programme research and innovation programme – Marie Skłodowska-Curie Actions Grant 841428 (F.L.), the Crohn's & Colitis Foundation Career Development Award 902590 (H.S.), and National Heart, Lung, and Blood Institute Grants K01 HL133530, P01HL151433–01 (M.A.L.-R. and Mark H. Ginsberg), HL139947 (Mark H. Ginsberg), and HL145454 (Z.F.). H.S. supervised the research; H.S. and F.L. conceived the study, designed experiments, interpreted data, and wrote the manuscript; F.L., H.S., B.T, Q.D., H.W., and W.Q. performed and analyzed experiments; Z.F., M.A.L.-R., and A.R.G. provided vital reagents and critical expertise.

Abbreviations used in this article:

EGFP	enhanced GFP
LPD	lamellipodin

MFI	mean fluorescence intensity
MLN	mesenteric lymph node
PLN	peripheral lymph node
pMSCV	murine stem cell virus plasmid
Tconv	conventional $CD4^+$ T
Treg	regulatory T

References

1. Hynes RO 2002. Integrins: bidirectional, allosteric signaling machines. Cell 110: 673–687. [PubMed: 12297042]
2. Hogg N, Patzak I, and Willenbrock F. 2011. The insider's guide to leukocyte integrin signalling and function. Nat. Rev. Immunol. 11: 416–426. [PubMed: 21597477]
3. Ley K, Laudanna C, Cybulsky MI, and Nourshargh S. 2007. Getting to the site of inflammation: the leukocyte adhesion cascade updated. Nat. Rev. Immunol. 7: 678–689. [PubMed: 17717539]
4. Vestweber D 2015. How leukocytes cross the vascular endothelium. Nat. Rev. Immunol. 15: 692–704. [PubMed: 26471775]
5. Springer TA, and Dustin ML. 2012. Integrin inside-out signaling and the immunological synapse. Curr. Opin. Cell Biol. 24: 107–115. [PubMed: 22129583]
6. Luo BH, Carman CV, and Springer TA. 2007. Structural basis of integrinregulation and signaling. Annu. Rev. Immunol. 25: 619–647. [PubMed: 17201681]
7. Takagi J, Petre BM, Walz T, and Springer TA. 2002. Global conformational rearrangements in integrin extracellular domains in outside-in and inside-out signaling. Cell 110: 599–611. [PubMed: 12230977]
8. Ley K, Rivera-Nieves J, Sandborn WJ, and Shattil S. 2016. Integrin-based therapeutics: biological basis, clinical use and new drugs. Nat. Rev. Drug Discov. 15: 173–183. [PubMed: 26822833]
9. Cox D, Brennan M, and Moran N. 2010. Integrins as therapeutic targets: lessons and opportunities. Nat. Rev. Drug Discov. 9: 804–820. [PubMed: 20885411]
10. Galkina E, and Ley K. 2007. Vascular adhesion molecules in atherosclerosis. Arterioscler. Thromb. Vasc. Biol. 27: 2292–2301. [PubMed: 17673705]
11. Abram CL, and Lowell CA. 2009. The ins and outs of leukocyte integrin signaling. Annu. Rev. Immunol. 27: 339–362. [PubMed: 19302044]
12. Shattil SJ, Kim C, and Ginsberg MH. 2010. The final steps of integrin activation: the end game. Nat. Rev. Mol. Cell Biol. 11: 288–300. [PubMed: 20308986]
13. Tadokoro S, Shattil SJ, Eto K, Tai V, Liddington RC, de Pereda JM,Ginsberg MH, and Calderwood DA. 2003. Talin binding to integrin beta tails: a final common step in integrin activation. Science 302: 103–106. [PubMed: 14526080]
14. Simonson WT, Franco SJ, and Huttenlocher A. 2006. Talin1 regulates TCR-mediated LFA-1 function. J. Immunol. 177: 7707–7714. [PubMed: 17114441]
15. Wernimont SA, Wiemer AJ, Bennin DA, Monkley SJ, Ludwig T, Critchley DR, and Huttenlocher A. 2011. Contact-dependent T cell activation and T cell stopping require talin1. J. Immunol. 187: 6256–6267. [PubMed: 22075696]
16. Sun H, Lagarrigue F, Gingras AR, Fan Z, Ley K, and Ginsberg MH. 2018. Transmission of integrin β7 transmembrane domain topology enables gut lymphoid tissue development. J. Cell Biol. 217: 1453–1465. [PubMed: 29535192]
17. Calderwood DA, Campbell ID, and Critchley DR. 2013. Talins and kindlins: partners in integrin-mediated adhesion. Nat. Rev. Mol. Cell Biol. 14: 503–517. [PubMed: 23860236]
18. Moser M, Legate KR, Zent R, and Fässler R. 2009. The tail of integrins, talin, and kindlins. Science 324: 895–899. [PubMed: 19443776]

19. Dedden D, Schumacher S, Kelley CF, Zacharias M, Biertümpfel C, Fässler R, and Mizuno N. 2019. The architecture of talin1 reveals an autoinhibition mechanism. Cell 179: 120–131.e13. [PubMed: 31539492]
20. Klann JE, Remedios KA, Kim SH, Metz PJ, Lopez J, Mack LA, Zheng Y, Ginsberg MH, Petrich BG, and Chang JT. 2017. Talin plays a critical role in the maintenance of the regulatory T cell pool. J. Immunol. 198: 4639–4651. [PubMed: 28515282]
21. Klann JE, Kim SH, Remedios KA, He Z, Metz PJ, Lopez J, Tysl T, Olvera JG, Ablack JN, Cantor JM, et al. 2018. Integrin activation controls regulatory T cell-mediated peripheral tolerance. J. Immunol. 200: 4012–4023. [PubMed: 29703862]
22. Lefort CT, Rossaint J, Moser M, Petrich BG, Zarbock A, Monkley SJ,Critchley DR, Ginsberg MH, Fässler R, and Ley K. 2012. Distinct roles for talin-1 and kindlin-3 in LFA-1 extension and affinity regulation. Blood 119: 4275–4282. [PubMed: 22431571]
23. Ishihara S, Nishikimi A, Umemoto E, Miyasaka M, Saegusa M, and Katagiri K.2015. Dual functions of Rap1 are crucial for T-cell homeostasis and prevention of spontaneous colitis.Nat. Commun. 6: 8982. [PubMed: 26634692]
24. Lee HS, Lim CJ, Puzon-McLaughlin W, Shattil SJ, and Ginsberg MH.2009. RIAM activates integrins by linking talin to ras GTPase membrane-targeting sequences. J. Biol. Chem. 284: 5119–5127. [PubMed: 19098287]
25. Lafuente EM, van Puijenbroek AA, Krause M, Carman CV, Freeman GJ, Berezovskaya A, Constantine E, Springer TA, Gertler FB, and Boussiotis VA. 2004. RIAM, an Ena/VASP and profilin ligand, interacts with Rap1-GTP and mediates Rap1-induced adhesion. Dev. Cell 7: 585–595. [PubMed: 15469846]
26. Petrich BG, Marchese P, Ruggeri ZM, Spiess S, Weichert RA, Ye F, Tiedt R, Skoda RC, Monkley SJ, Critchley DR, and Ginsberg MH. 2007. Talin is required for integrin-mediated platelet function in hemostasis and thrombosis. J. Exp. Med. 204: 3103–3111. [PubMed: 18086863]
27. Nieswandt B, Moser M, Pleines I, Varga-Szabo D, Monkley S, Critchley D, and Fässler R. 2007. Loss of talin1 in platelets abrogates integrin activation, platelet aggregation, and thrombus formation in vitro and in vivo. J. Exp. Med. 204: 3113–3118. [PubMed: 18086864]
28. Klapproth S, Sperandio M, Pinheiro EM, Prünster M, Soehnlein O, Gertler FB, Fässler R, and Moser M. 2015. Loss of the Rap1 effector RIAM results in leukocyte adhesion deficiency due to impaired β2 integrin function in mice. Blood 126: 2704–2712. [PubMed: 26337492]
29. Su W, Wynne J, Pinheiro EM, Strazza M, Mor A, Montenont E, Berger J, Paul DS, Bergmeier W, Gertler FB, and Philips MR. 2015. Rap1 and its effector RIAM are required for lymphocyte trafficking. Blood 126: 2695–2703. [PubMed: 26324702]
30. Stritt S, Wolf K, Lorenz V, Vögtle T, Gupta S, Bösl MR, and Nieswandt B. 2015. Rap1-GTP-interacting adaptor molecule (RIAM) is dispensable for platelet integrin activation and function in mice. Blood 125: 219–222. [PubMed: 25336629]
31. Lagarrigue F, Gertler FB, Ginsberg MH, and Cantor JM. 2017. Cutting edge: loss of T cell RIAM precludes conjugate formation with APC and prevents immune-mediated diabetes. J. Immunol. 198: 3410–3415. [PubMed: 28348273]
32. Sun H, Lagarrigue F, Wang H, Fan Z, Lopez-Ramirez MA, Chang JT, and Ginsberg MH. 2021. Distinct integrin activation pathways for effector and regulatory T cell trafficking and function. J. Exp. Med. 218: e20201524. [PubMed: 33104169]
33. Goult BT, Bouaouina M, Elliott PR, Bate N, Patel B, Gingras AR, Grossmann JG, Roberts GC, Calderwood DA, Critchley DR, and Barsukov IL. 2010. Structure of a double ubiquitin-like domain in the talin head: a role in integrin activation. EMBO J. 29: 1069–1080. [PubMed: 20150896]
34. Zhu L, Yang J, Bromberger T, Holly A, Lu F, Liu H, Sun K, Klapproth S, Hirbawi J, Byzova TV, et al. 2017. Structure of Rap1b bound to talin reveals a pathway for triggering integrin activation. Nat. Commun. 8: 1744. [PubMed: 29170462]
35. Lagarrigue F, Gingras AR, Paul DS, Valadez AJ, Cuevas MN, Sun H, Lopez-Ramirez MA, Goult BT, Shattil SJ, Bergmeier W, and Ginsberg MH. 2018. Rap1 binding to the talin 1 F0 domain makes a minimal contribution to murine platelet GPIIb-IIIa activation. Blood Adv. 2: 2358–2368. [PubMed: 30242097]

36. Bromberger T, Klapproth S, Rohwedder I, Zhu L, Mittmann L, Reichel CA, Sperandio M, Qin J, and Moser M. 2018. Direct Rap1/talin1 interaction regulates platelet and neutrophil integrin activity in mice. Blood 132: 2754–2762. [PubMed: 30442677]
37. Gingras AR, Lagarrigue F, Cuevas MN, Valadez AJ, Zorovich M, McLaughlin W, Lopez-Ramirez MA, Seban N, Ley K, Kiosses WB, and Ginsberg MH. 2019. Rap1 binding and a lipid-dependent helix in talin F1 domain promote integrin activation in tandem. J. Cell Biol. 218: 1799–1809. [PubMed: 30988001]
38. Lagarrigue F, Paul DS, Gingras AR, Valadez AJ, Sun H, Lin J, Cuevas MN, Ablack JN, Lopez-Ramirez MA, Bergmeier W, and Ginsberg MH. 2020. Talin-1 is the principal platelet Rap1 effector of integrin activation. Blood 136: 1180–1190. [PubMed: 32518959]
39. Liao Z, Gingras AR, Lagarrigue F, Ginsberg MH, and Shattil SJ. 2021. Optogenetics-based localization of talin to the plasma membrane promotes activation of β3 integrins. J. Biol. Chem. 296: 100675. [PubMed: 33865854]
40. Haling JR, Monkley SJ, Critchley DR, and Petrich BG. 2011. Talin-dependent integrin activation is required for fibrin clot retraction by platelets. Blood 117: 1719–1722. [PubMed: 20971947]
41. Law AL, Vehlow A, Kotini M, Dodgson L, Soong D, Theveneau E, Bodo C, Taylor E, Navarro C, Perera U, et al. 2013. Lamellipodin and the Scar/WAVE complex cooperate to promote cell migration in vivo. J. Cell Biol. 203: 673–689. [PubMed: 24247431]
42. Lee PP, Fitzpatrick DR, Beard C, Jessup HK, Lehar S, Makar KW, Pérez-Melgosa M, Sweetser MT, Schlissel MS, Nguyen S, et al. 2001. A critical role for Dnmt1 and DNA methylation in T cell development, function, and survival. Immunity 15: 763–774. [PubMed: 11728338]
43. Rubtsov YP, Rasmussen JP, Chi EY, Fontenot J, Castelli L, Ye X, Treuting P, Siewe L, Roers A, Henderson WR Jr., et al. 2008. Regulatory T cell-derived interleukin-10 limits inflammation at environmental interfaces. Immunity 28: 546–558. [PubMed: 18387831]
44. Sun H, Liu J, Zheng Y, Pan Y, Zhang K, and Chen J. 2014. Distinct chemokine signaling regulates integrin ligand specificity to dictate tissue-specific lymphocyte homing. Dev. Cell 30: 61–70. [PubMed: 24954024]
45. Rose DM, Cardarelli PM, Cobb RR, and Ginsberg MH. 2000. Soluble VCAM-1 binding to a4 integrins is cell-type specific and activation dependent and is disrupted during apoptosis in T cells. Blood 95: 602–609. [PubMed: 10627469]
46. Manevich-Mendelson E, Grabovsky V, Feigelson SW, Cinamon G, Gore Y, Goverse G, Monkley SJ, Margalit R, Melamed D, Mebius RE, et al. 2010. Talin1 is required for integrin-dependent B lymphocyte homing to lymph nodes and the bone marrow but not for follicular B-cell maturation in the spleen. Blood 116: 5907–5918. [PubMed: 20923969]
47. Lagarrigue F, Kim C, and Ginsberg MH. 2016. The Rap1-RIAM-talin axis of integrin activation and blood cell function. Blood 128: 479–487. [PubMed: 27207789]
48. Patsoukis N, Bardhan K, Weaver JD, Sari D, Torres-Gomez A, Li L, Strauss L, Lafuente EM, and Boussiotis VA. 2017. The adaptor molecule RIAM integrates signaling events critical for integrin-mediated control of immune function and cancer progression. Sci. Signal. 10: eaam8298. [PubMed: 28831022]
49. Wegener KL, Partridge AW, Han J, Pickford AR, Liddington RC, Ginsberg MH, and Campbell ID. 2007. Structural basis of integrin activation by talin. Cell 128: 171–182. [PubMed: 17218263]
50. von Andrian UH, and Mempel TR. 2003. Homing and cellular traffic in lymph nodes. Nat. Rev. Immunol. 3: 867–878. [PubMed: 14668803]
51. Nolte MA, Hamann A, Kraal G, and Mebius RE. 2002. The strict regulation of lymphocyte migration to splenic white pulp does not involve common homing receptors. Immunology 106: 299–307. [PubMed: 12100717]
52. Katagiri K, Maeda A, Shimonaka M, and Kinashi T. 2003. RAPL, a Rap1-binding molecule that mediates Rap1-induced adhesion through spatial regulation of LFA-1. Nat. Immunol. 4: 741–748. [PubMed: 12845325]
53. Katagiri K, Ohnishi N, Kabashima K, Iyoda T, Takeda N, Shinkai Y, Inaba K, and Kinashi T. 2004. Crucial functions of the Rap1 effector molecule RAPL in lymphocyte and dendritic cell trafficking. Nat. Immunol. 5: 1045–1051. [PubMed: 15361866]

54. Kondo N, Ueda Y, Kita T, Ozawa M, Tomiyama T, Yasuda K, Lim DS, and Kinashi T. 2017. NDR1-dependent regulation of kindlin-3 controls high-affinity LFA-1 binding and immune synapse organization. Mol. Cell. Biol. 37: e00424–16. [PubMed: 28137909]

55. Parmo-Cabañas M, García-Bernal D, García-Verdugo R, Kremer L, Márquez G, and Teixidó J. 2007. Intracellular signaling required for CCL25-stimulated T cell adhesion mediated by the integrin $\alpha_4\beta_1$. J. Leukoc. Biol. 82: 380–391. [PubMed: 17510295]

56. Bromberger T, Klapproth S, Rohwedder I, Weber J, Pick R, Mittmann L, Min-Weißenhorn SJ, Reichel CA, Scheiermann C, Sperandio M, and Moser M. 2021. Binding of Rap1 and Riam to talin1 fine-tune β2 integrin activity during leukocyte trafficking. Front. Immunol. 12: 702345. [PubMed: 34489950]

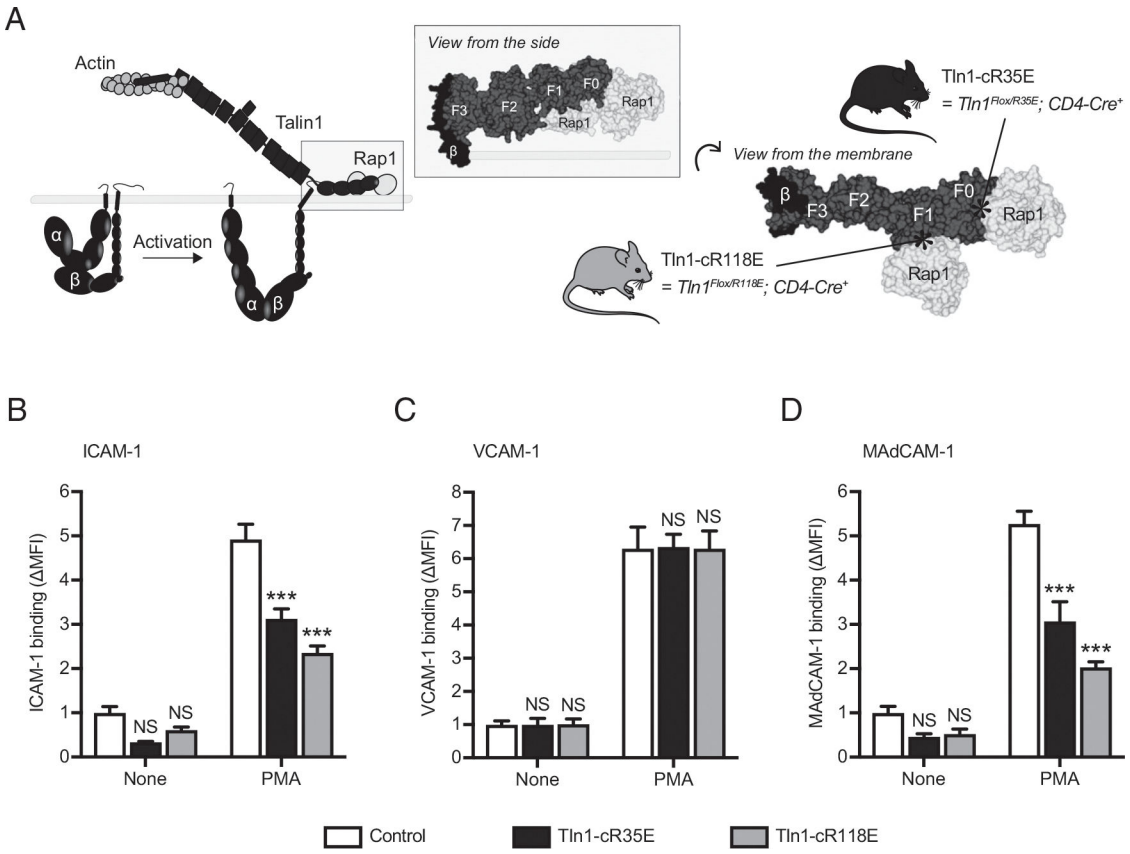

FIGURE 1.

Rap1 binding to talin1 F0 or F1 subdomain contributes to integrin activation in $CD4^+$ T cells and Treg cells. (**A**) Diagram depicting the role of talin1 in integrin activation. Mutations R35E and R118E in talin1 block Rap1 binding to F0 and F1 subdomains, respectively. (**B–D**) Binding of control and Tln1-cR35E or Tln1-cR118E mutant $CD4^+$ T cells to soluble integrin ligands. Cellular stimulation was achieved with 100 nM PMA. Data represent mean ± SEM ($n = 4$ mice), normalized to the unstimulated control condition. Statistical significance in (B–D) was measured against the WT control T cells. One-way ANOVA with Bonferroni post hoc test. ***$p < 0.001$.

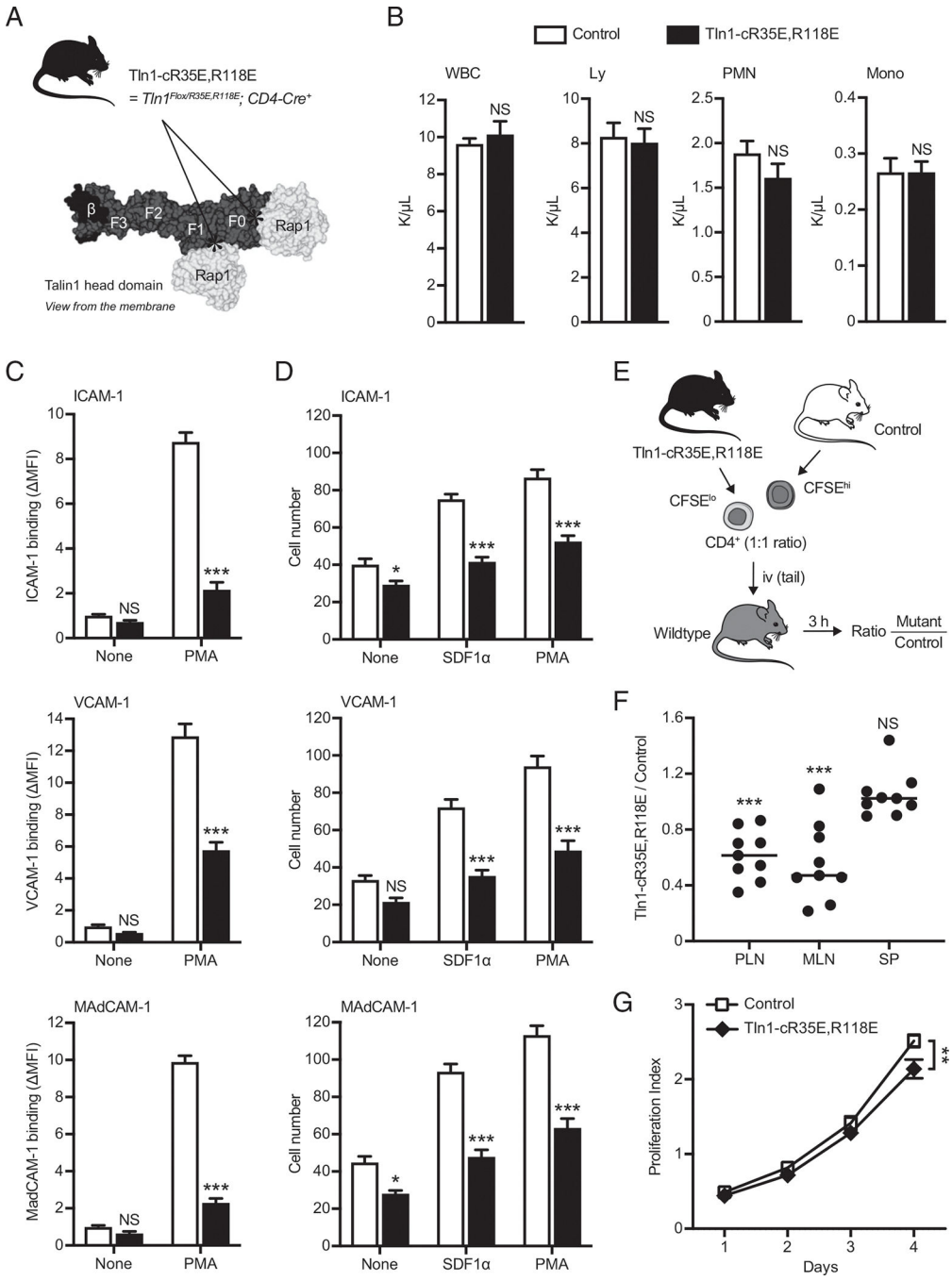

FIGURE 2.

Blockade of Rap1 binding to both F0 and F1 subdomains in talin1 prevents integrin activation in CD4$^+$ T cells. (**A**) Both R35E and R118E mutations in talin1 F0 and F1 subdomains, respectively, prevent Rap1–talin1 interaction. (**B**) Peripheral blood cell counts of Tln1-cR35E,R118E mice. Values are mean ± SEM (n = 6 mice). Two-tailed t test; no significant differences were observed. PMN, polymorphonuclear neutrophils; Ly, lymphocytes; Mono, monocytes. (**C**) Binding of control or Tln1-cR35E,R118E mutant CD4$^+$ T cells to soluble integrin ligands. Cells were stimulated with 100 nM PMA. Data

represent mean ± SEM (n = 10 mice), normalized to the unstimulated control condition. Two-way ANOVA with Bonferroni post hoc test.***p < 0.001.(**D**) Static adhesion of control or Tln1-cR35E,R118E mutant CD4$^+$ T cells to integrin ligands. Cells were stimulated with 1μg/ml SDF1α or 100nM PMA. The number of arrested adherent cells was plotted. Data are mean ± SEM (n = 6mice). Two-way ANOVA with Bonferroni post hoc test.*p < 0.05,***p < 0.001.(**E** and **F**) In vivo competitive homing of Tln1-cR35E,R118E mutant CD4$^+$ T cells to different lymphoid tissues. CD4$^+$ T cells were isolated from either control or Tln1-cR35E,R118E mice, differentially labeled, and mixed before injection into C57BL/6 mice. The ratio of Tln1-cR35E,R118E mutant to control CD4$^+$ T cells was determined by flow cytometry from PLNs and MLNs or spleens 3h after injection. Data represent mean ± SEM (n = 9 mice). One-way ANOVA with Bonferroni post hoc test. ***p < 0.001. (**G**) In vitro cell proliferation assay. CD4$^+$ T cells were isolated from spleens and labeled with CFSE before stimulation with plate-bound anti-CD3/CD28 mAb for 4 d at 37°C. Proliferation index was plotted. Data represent mean ± SEM (n = 4 mice). Two-way ANOVA with Bonferroni post hoc test. **p < 0.01. (B–E and G) Statistical significance was measured against the WT control T cells or mice.

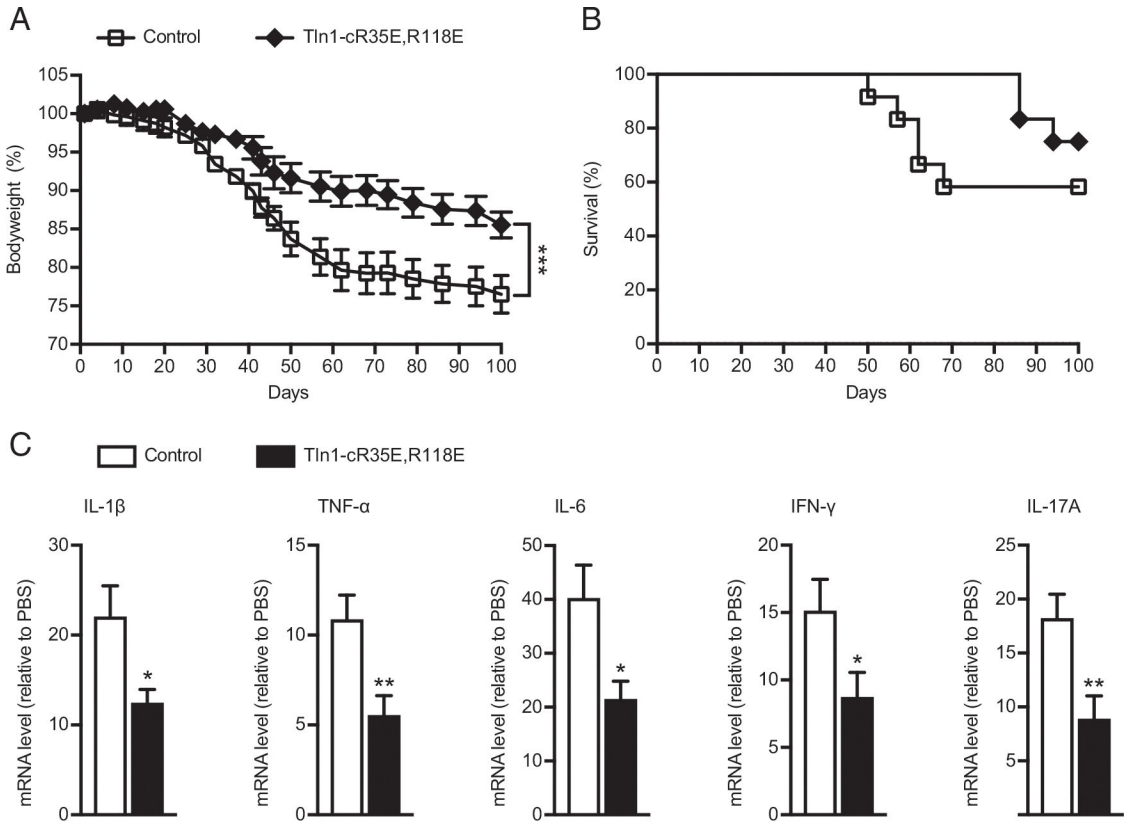

FIGURE 3.

Loss of interaction between Rap1 and talin1 protects mice from colitis. Conventional T cells (10^6) from WT or Tln1-cR35E,R118E mice were adoptively transferred into *Rag1*$^{-/-}$ mice. (**A**) Changes in body weight are plotted. Values are normalized as a percentage of the original weight. Two-way ANOVA with Bonferroni post hoc test. ***$p < 0.001$. (**B**) Percentage survival. Data represent mean ± SEM ($n = 12$ mice). Gehan-Breslow-Wilcoxon test. (**C**) mRNA expression of IL-1β, TNF-α, IL-6, IFN-γ, and IL-17A in distal colon tissues from individual groups of mice relative to PBS-injected control mice at Day 100. Results are normalized to expression of GAPDH. Mean ± SEM are plotted. Two-tailed *t* test; *$p < 0.05$, **$p < 0.01$. (A–C) Statistical significance was measured against the WT control T cells or mice.

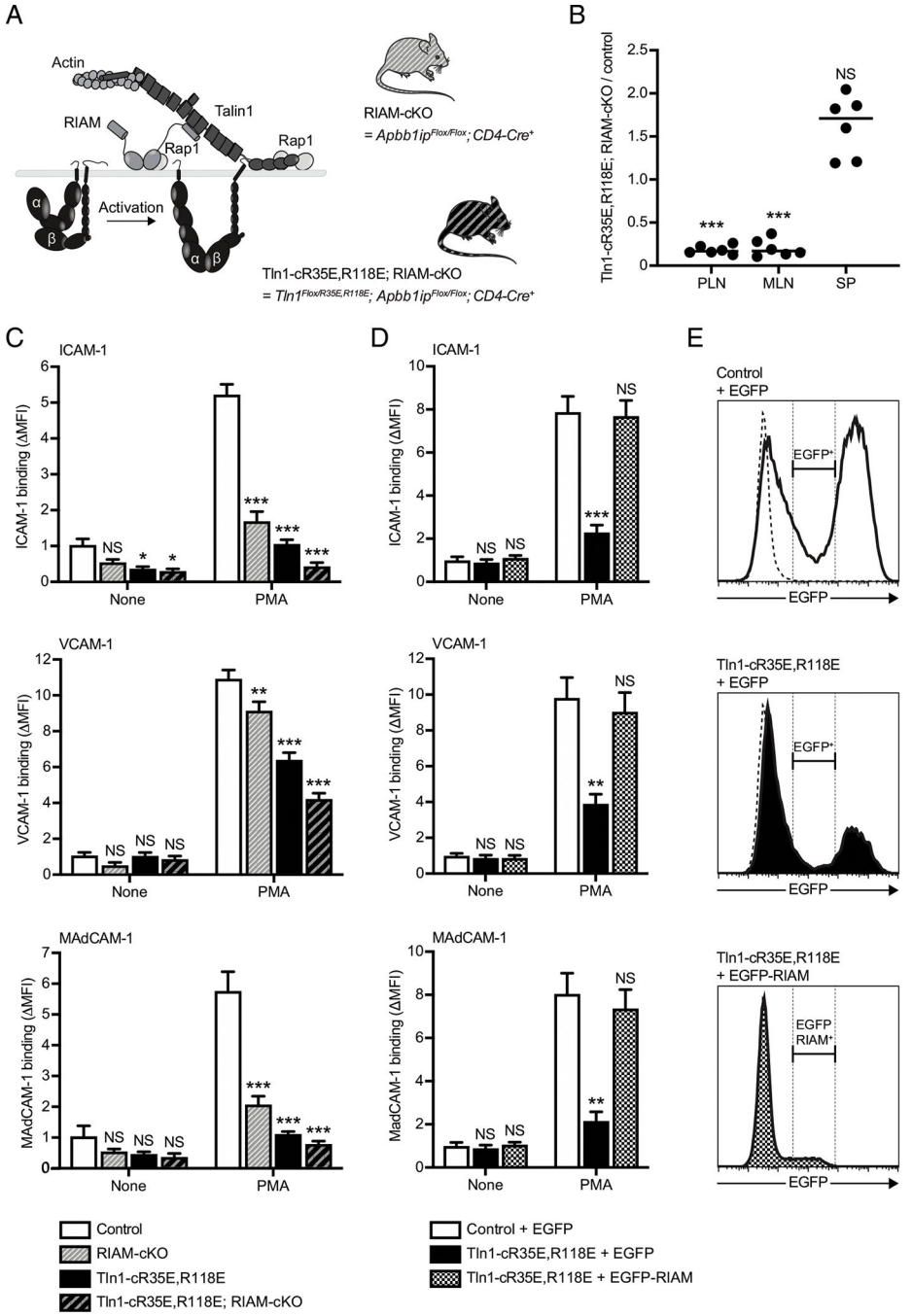

FIGURE 4.

Rap1–talin1 direct interaction synergizes with Rap1–RIAM–talin1 to mediate integrin activation in CD4$^+$ T cells. (**A**) RIAM functions as a Rap1 effector that recruits talin1 to the plasma membrane, in parallel to Rap1 binding to talin1, to enable its interaction with the integrin β cytoplasmic tail. (**B**) In vivo competitive homing of Tln1-cR35E,R118E; RIAM-cKO CD4$^+$ T cells to different lymphoid tissues. CD4$^+$ T cells were isolated from either control or Tln1-cR35E,R118E; RIAM-cKO mice, differentially labeled, and mixed before injection into C57BL/6 mice. The ratio of Tln1-cR35E,R118E; RIAM-cKO mutant to

control $CD4^+$ T cells was determined by flow cytometry from PLNs and MLNs or spleens (SP) 3 h after injection. Data represent mean ± SEM ($n = 6$ mice). One-way ANOVA with Bonferroni post hoc test. ***$p < 0.001$. (**C**) Binding of control, Tln1-cR35E,R118E, or Tln1-cR35E,R118E; RIAM-cKO mutant $CD4^+$ T cells to soluble integrin ligands. Cells were stimulated with 100 nM PMA. Data represent mean ± SEM ($n = 4$ mice), normalized to the unstimulated control condition. Two-way ANOVA with Bonferroni post hoc test. *$p < 0.05$, **$p < 0.01$, ***$p < 0.001$. (**D** and **E**) $CD4^+$ T cells isolated from control or Tln1-cR35E,R118E mice were transduced with retroviruses encoding either EGFP-tagged RIAM or EGFP alone. Integrin activation in $EGFP^+$ cells was analyzed by flow cytometry. (D) The level of EGFP expression was determined at 3 d after transduction. (E) Binding of transduced $CD4^+$ T cells to soluble integrin ligands. Cells were stimulated with 100 nM PMA. Data represent mean ± SEM ($n = 4$ mice). Two-way ANOVA with Bonferroni post hoc test. **$p < 0.01$, ***$p < 0.001$. (B–D) Statistical significance was measured against the WT control T cells.

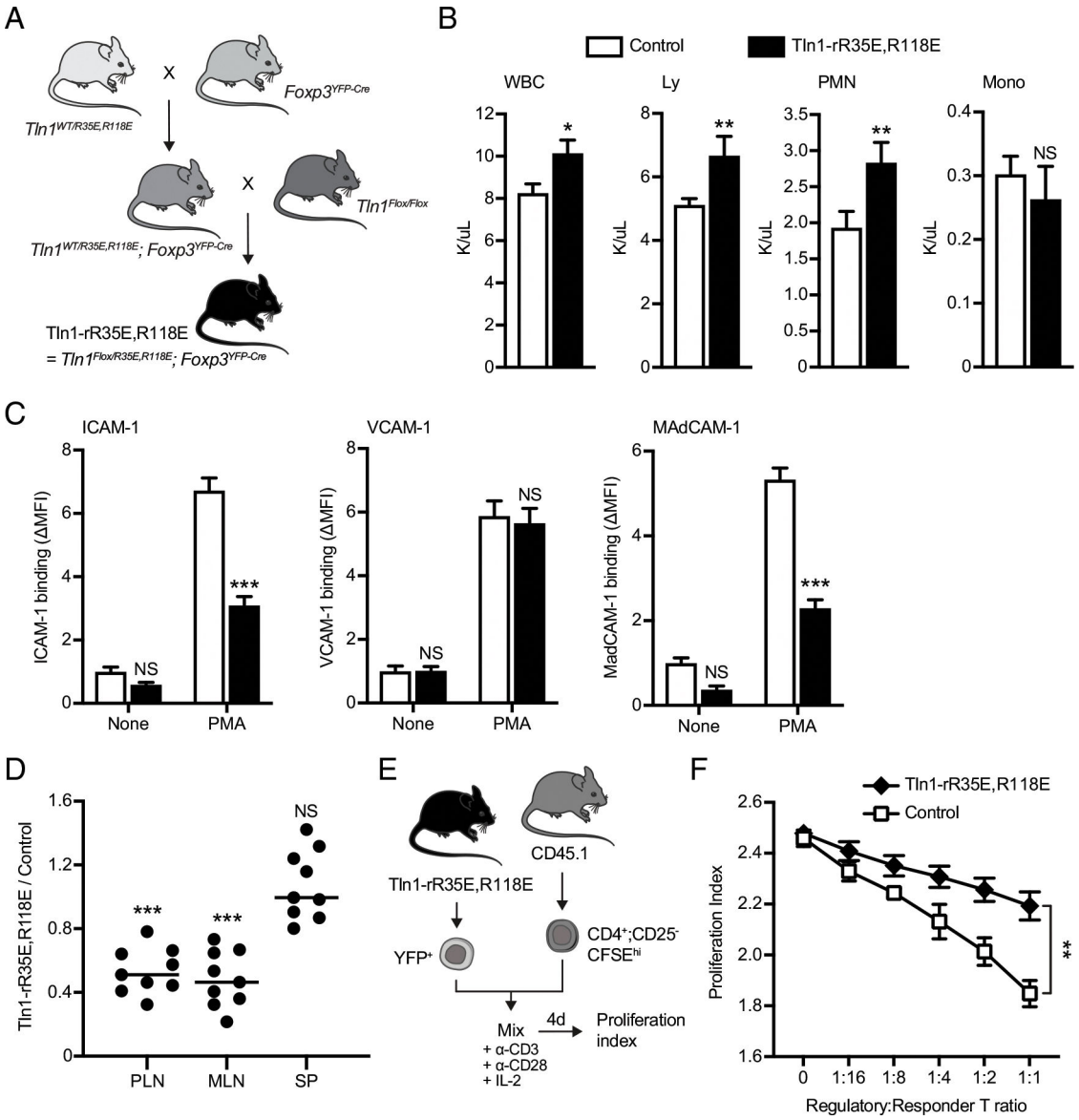

FIGURE 5.

Rap1 binding to talin1 participates to activate integrins in Treg cells. (**A**) Mouse breeding strategy to selectively restrict the expression of talin1(R35E,R118E) in Treg cells. (**B**) Peripheral blood cell counts of Tln1-rR35E,R118E mice. Values are mean ± SEM ($n = 6$ mice). Two-tailed t test; $*p < 0.05$, $**p < 0.01$. PMN, polymorphonuclear neutrophils; Ly, lymphocytes; Mono, monocytes. (**C**) Binding of control or Tln1-rR35E,R118E mutant Treg cells to soluble integrin ligands. Cells were stimulated with 100 nM PMA. Data represent mean ± SEM ($n = 8$ mice), normalized to the unstimulated control condition. Two-way ANOVA with Bonferroni post hoc test. $***p < 0.001$. (**D**) In vivo competitive homing of Tln1-rR35E,R118E mutant Treg cells to different lymphoid tissues. Treg cells were isolated from either control or Tln1-rR35E,R118E mice, differentially labeled, and mixed before injection into C57BL/6 mice. The ratio of Tln1-rR35E,R118E mutant to control Treg cells was determined by flow cytometry from PLNs and MLNs or spleens (SP) 3 h after injection.

Data represent mean ± SEM (n = 9 mice). One-way ANOVA with Bonferroni post hoc test. ***$p < 0.001$. (**E** and **F**) Treg cell suppressive activity. Treg cells isolated from CD45.2 congenic control or Tln1-rR35E,R118E mice were mixed with responder T cells at the indicated Treg/responder cell ratios. Responder cells were CFSE-labeled $CD4^+CD25^-$ naïve T cells isolated from CD45.1 congenic C57BL/6 mice and activated by anti-CD3 (5 μg/ml), anti-CD28 (5 μg/ml), and IL-2. $CFSE^+$ populations gated on $CD45.1^+$ cells were analyzed by flow cytometry at Day 4 to determine the proliferation index using FlowJo software (n = 3 mice). Two-way ANOVA with Bonferroni post hoc test. **$p < 0.01$. (B–D and F) Statistical significance was measured against the WT control T cells or mice.

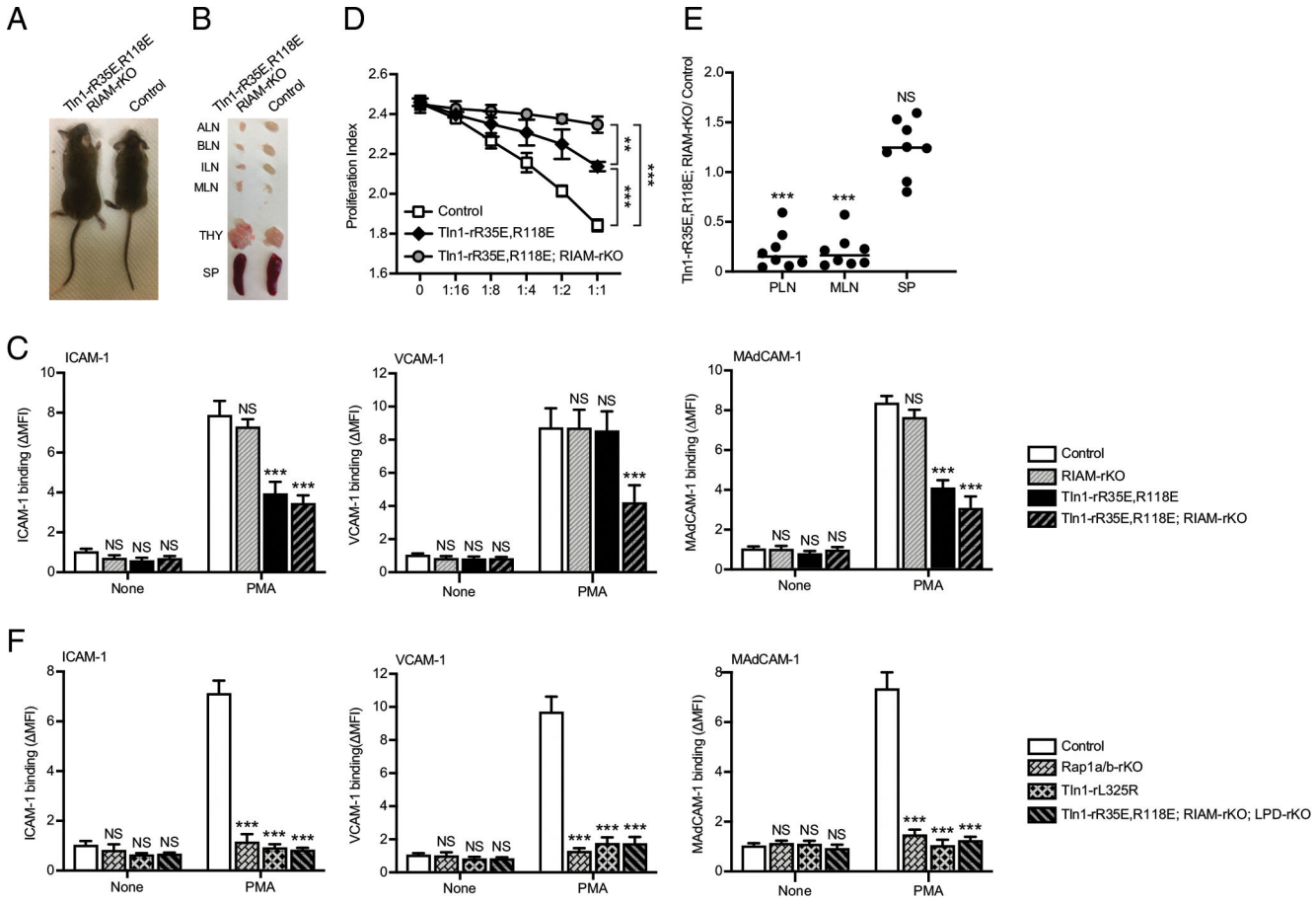

FIGURE 6.

Both LPD and Rap1 binding to talin1 contribute to activate integrins in Treg cells. (**A** and **B**) Representative morphology (A) and lymphoid tissues (B) of Tln1-rR35E,R118E; RIAM-rKO mice. ALN, aortic lymph nodes; BLN, brachial lymph nodes; ILN, inguinal lymph nodes; SP, spleen; THY, thymus. (**C**) Binding of control, RIAM-rKO, Tln1-rR35E,R118E, or Tln1-rR35E,R118E; RIAM-rKO mutant Treg cells to soluble integrin ligands. Cells were stimulated with 100 nM PMA. Data represent mean ± SEM (n = 4 mice), normalized to the unstimulated control condition. Two-way ANOVA with Bonferroni post hoc test. ***$p < 0.001$. (**D**) Treg cell suppressive activity. Treg cells isolated from CD45.2 congenic control or Tln1-rR35E,R118E; RIAM-rKO mice were mixed with responder T cells at the indicated Treg/responder cell ratios. Responder cells were CFSE-labeled $CD4^+CD25^-$ naive T cells isolated from CD45.1 congenic C57BL/6 mice and activated by anti-CD3 (5 μg/ml), anti-CD28 (5 μg/ml), and IL-2. $CFSE^+$ populations gated on $CD45.1^+$ cells were analyzed by flow cytometry at Day 4 to determine the proliferation index using FlowJo software (n = 4 mice). Two-way ANOVA with Bonferroni post hoc test. **$p < 0.01$, ***$p < 0.001$. (**E**) In vivo competitive homing of Tln1-rR35E,R118E; RIAM-rKO Treg cells to different lymphoid tissues. Treg cells were isolated from either control or Tln1-rR35E,R118E; RIAM-rKO mice, differentially labeled, and mixed before injection into C57BL/6 mice. The ratio of Tln1-rR35E,R118E; RIAM-rKO mutant to control Treg cells was determined by flow cytometry from PLNs and MLNs or spleens 3 h after injection. Data represent mean ± SEM

(n = 8 mice). One-way ANOVA with Bonferroni post hoc test. ***$p < 0.001$. (**F**) Binding of control, Tln1-rL325R, or Tln1-rR35E,R118E; RIAM-rKO; LPD-rKO mutant Treg cells to soluble integrin ligands. Cells were stimulated with 100 nM PMA. Data represent mean ± SEM (n = 4 mice). Two-way ANOVA with Bonferroni post hoc test. ***$p < 0.001$. (C–F) Statistical significance was measured against the WT control T cells.